Hypervalent zinc(I) complexes with an *NNNN*-macrocycle: C–H bond activation across the zinc(I)–zinc(I) bond†

Pritam Mahawar,[a] Thayalan Rajeshkumar,[b] Thomas P. Spaniol,[a] Laurent Maron [ID][b] and Jun Okuda [ID] *[a]

Hetero- and homoleptic dinuclear zinc(I) complexes containing the macrocycle Me$_4$TACD (*N,N′,N″,N‴*-1,4,7,10-tetramethylcyclodo-decane) were prepared; the heteroleptic complex [(Me$_4$TACD)Zn–ZnCp*]$^+$ reacted with activated hydrocarbons R–H (R = CH$_2$CN, C≡CPh) to give the corresponding hydrocarbyl zinc(II) complexes [(Me$_4$TACD)ZnR]$^+$.

The discovery of decamethyldizincocene Cp*Zn–ZnCp* (Cp* = η^5-C$_5$Me$_5$) by Carmona *et al.* in 2004[1] has prompted the isolation of other complexes featuring the remarkable zinc(I)–zinc(I) σ-bond. On the one hand, neutral zinc(I) analogs containing a L$_l$X-type ligand (L = two-electron, X = one-electron ligand)[2a] such as bulky aryl (*l* = 0)[3] and β-diketiminato (*l* = 1)[4] became known, on the other hand protonolysis or oxidation of Cp*Zn–ZnCp* allowed the synthesis of mono(cations) of the type [((L$_3$)Zn–ZnCp*)]$^+$ (ref. 5) or dicationic complexes [(L$_3$)Zn–Zn(L$_3$)]$^{2+}$(L = THF, DMAP).[6] Regarding zinc as a main group element with filled 3d^{10} shell,[2b] the valence electron count of zinc in all these complexes does not exceed 8 electrons.[2,7] Recently, we have reported that the heteroleptic zinc(I) cation [[(TEEDA)(thf)Zn–ZnCp*]$^+$[BAr$_4$^{F}]$^-$ (TEEDA = *N,N,N′,N′*-tetraethylethylenediamine; Ar^F = 3,5-((CF$_3$)$_2$C$_6$H$_3$)) can undergo a heterolytic dihydrogen cleavage.[8] As recently suggested for the reactivity of diberyllocene,[9] main group metal–metal bonds can be polarized, so for decamethyldizincocene a resonance structure [Cp*Zn(II)]$^+$ ← [Zn(0)Cp*]$^-$ can be implied, accounting for some of the reactivity patterns (redox disproportionation) observed.[10] We wondered whether introducing hypervalency[7] at the zinc(I) center (with

formal valence electron count higher than 8) would result in a higher reactivity of the zinc(I)–zinc(I) bond. Here we report on the preparation of both homo- and heteroleptic zinc(I) cations that contain the L$_4$-type macrocycle Me$_4$TACD (*N,N′,N″,N‴*-1,4,7,10-tetramethylcyclododecane).[11] The heteroleptic zinc(I) cation was found to undergo a heterolytic C–H bond activation of acetonitrile and phenylacetylene.[10,12]

The versatile macrocyclic ligand Me$_4$TACD is capable of coordinating s-,[13] and p-block[14] metal cations including low-valent triele cations Ga(I), In(I) and Tl(I). Thus, stoichiometric reaction of Cp*Zn–ZnCp* with the borate salt of the protonated Me$_4$TACD [(Me$_4$TACD)H][BAr$_4$^{Me}][15] (BAr$_4$^{Me} = [B{3,5-(CH$_3$)$_2$-C$_6$H$_3$}$_4$]$^-$) in THF at room temperature for one hour afforded the heteroleptic zinc(I) monocation [(Me$_4$TACD)Zn–ZnCp*][BAr$_4$^{Me}] (**1**) in 90% yield with the elimination of one equivalent of Cp*H. Colorless compound **1** is stable under argon at room temperature and is soluble in THF, acetonitrile, and dichloromethane (Scheme 1).

Compound **1** was characterized in solution using multi-nuclear NMR spectroscopy, including ^{1}H, ^{13}C, and ^{11}B, and in the solid state using single crystal X-ray diffraction. The ^{1}H NMR spectra indicate η^5-Cp* coordination, displaying a characteristic single peak for all methyl groups of Cp* at δ 2.02 ppm and confirmed the ligand/borate ratio of 1:1. The diastereotopic CH$_2$CH$_2$ protons of the Me$_4$TACD ligand appear as multiplets of AA′BB′ spin system in the range of δ 2.14–2.31 ppm, as commonly observed for the coordinated Me$_4$TACD ligand.[14] The ^{13}C{^{1}H} NMR spectrum revealed two signals for the Cp* methyl and ring carbons at δ 10.5 and δ 108.4 ppm, respectively, along with the peaks for the Me$_4$TACD ligand and

[a] *Institute of Inorganic Chemistry, RWTH Aachen University, Landoltweg 1, 52056 Aachen, Germany. E-mail: jun.okuda@ac.rwth-aachen.de*

[b] *CNRS, INSA, UPS, UMR 5215, LPCNO, Université de Toulouse, 135 Avenue de Rangueil, 31077 Toulouse, France. E-mail: laurent.maron@irsamc.ups-tlse.fr*
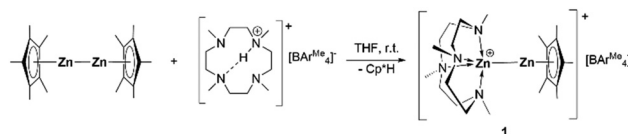
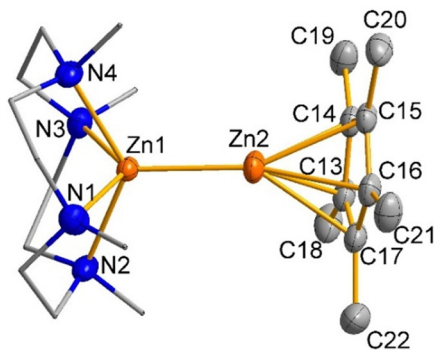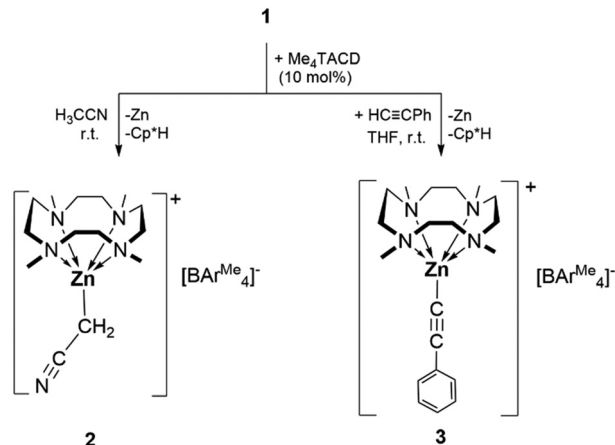Scheme 1 Synthesis of [(Me$_4$TACD)Zn–ZnCp*][BAr$_4$^{Me}] (**1**).

Fig. 1 Cationic part of the molecular structure of compound **1**. Selected interatomic distances [Å] and angles [°]: Zn1–Zn2 2.3510(3), Zn1–N1 2.2388(17), Zn1–N2 2.2177(15), Zn1–N3 2.2550(15), Zn1–N4 2.2181(15), Zn1–C13 2.3484(18), Zn1–C14 2.3168(18), Zn1–C15 2.2779(17), Zn1–C16 2.2889(18), Zn1–C17 2.3275(18), N1–Zn1–N2 80.40(6), N1–Zn1–N3 130.33(6), N1–Zn1–N4 79.98(6), N1–Zn1–Zn2 115.79(4), N2–Zn1–Zn2 112.12(4), N3–Zn1–Zn2 113.83(4), N4–Zn1–Zn2 117.99(4).

Scheme 2 Reaction of [Me₄TACDZn–ZnCp*][BAr₄^Me] (**1**) with activated hydrocarbons.

borate counter-ion. Compound **1** crystallizes in the monoclinic space group $P2_1/n$ with one ion pair per asymmetric unit. The structure of the molecular cation is depicted in Fig. 1 (see ESI† for details). The cationic penta-coordinate zinc center is positioned above the N₄-basal plane of the Me₄TACD ligand with the Zn–N$_{(centroid)}$ bond distance of 0.9416(6) Å, which is consistent with the Zn–N$_{(centroid)}$ bond distance (0.9371(15) Å) in the zinc(II) hydride cation [(Me₄TACD)ZnH][HBPh₃].[16] The zinc–zinc distance of 2.3510(3) Å is marginally longer than the reported value for heteroleptic Zn(I) monocations [(Et₂O)₃Zn–ZnCp*][BAr₄^F] (2.324(2) Å)[5] and [(TEEDA)Zn–ZnCp*][BAr₄^F] (2.3253(15) Å).[8] The enhanced polarization effect caused by the increased coordination number and asymmetrical ligand environment causes the zinc–zinc bond distance to be longer than in Cp*Zn–ZnCp* with 2.302(1) Å.[1]

Compound **1** shows a slight slipping of the Cp* ring from η⁵-coordination to Zn1, with the metal atom's projection displaced from the ring's centroid by 0.072 Å. The Zn1–Cp*$_{(centroid)}$ distance (1.971 Å) lies within the range of the Zn1–Cp*$_{(centroid)}$ bond distances in heteroleptic zinc(I) complexes [(TEEDA)Zn–ZnCp*][BAr₄^F] (1.954 Å)[8] and [(HC{C(Me)NDipp}₂)Zn–ZnCp*] (1.9215(3) Å).[17] This slipped coordination results in the non-linear alignment of the Zn2–Zn1–Cp*$_{(centroid)}$ bond angle of 164.75(1)° in **1**.

Reactivity studies of zinc(I) complexes toward activated hydrocarbons are scarce,[10] although reactions with phenylacetylene have been studied.[10a–c] While the zinc(I) cation **1** is kinetically robust in acetonitrile for at least 12 h, in the presence of 10 mol% of Me₄TACD, the formation of a grey precipitate was observed within 5 min and zinc(II) cyanomethanide [(Me₄TACD)Zn(CH₂CN)][BAr₄^Me] (**2**) was isolated from the supernatant in 85% yield (Scheme 2). Formation of **2** can be interpreted as a product of oxidative C–H bond addition across the Zn–Zn bond of **1**, presumably also forming unstable [Cp*ZnH],[18] which is known to decompose via reductive elimination to form the observed byproducts Cp*H and metallic zinc. Compound **2** can also be synthesized in THF using 2
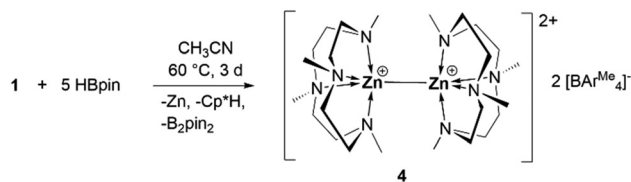
equivalents of acetonitrile in the presence of 10 mol% of Me₄TACD. Likewise, in the presence of 10 mol% of Me₄TACD, the reaction of compound **1** with phenylacetylene in THF at room temperature gave the zinc(II) acetylide complex [(Me₄TACD)ZnC≡CPh][BAr₄^Me] (**3**) in 90% isolated yield (Scheme 2). The precise role of Me₄TACD is unclear, it may act as a Brønsted base in these reactions. Compounds **2** and **3** are soluble in THF, acetonitrile, and dichloromethane and are stable at room temperature under argon. Compounds **2** and **3** were characterized using multinuclear NMR spectroscopy (¹H, ¹³C, ¹¹B) in the solution state. The solid-state characterization was performed using single-crystal XRD and IR spectroscopy. In the ¹H and ¹³C{¹H} NMR spectra of compound **2** the characteristic peaks for the CH₂CN protons appear at δ 0.52 ppm and δ −14.3 ppm, respectively. For the acetylide compound **3** the ¹³C{¹H} NMR spectrum shows the characteristic peaks for the acetylenic carbon atoms at δ 109.0 and 107.8 ppm. All peaks of the Me₄TACD ligands in compounds **2** and **3** are downfield shifted compared to those of **1**, due to the increase in oxidation number of zinc from +1 in compound **1** to +2 in compounds **2** and **3**.

Single crystal X-ray diffraction studies revealed the monomeric structure of compounds **2** and **3** (see ESI†). The coordination of the Me₄TACD ligand at the cationic zinc(II) center in compounds **2** and **3** is comparatively stronger than in precursor **1** with zinc(I) cation which can be seen by the decrease in the Zn–N$_{(centroid)}$ bond distance (0.8856(16) Å for **2** and 0. 8776(9) Å for **3**) from 0.9416(6) (for **1**). The Zn–CH₂ bond distance in compound **2** of 2.025(3) Å is comparable to the Zn–CH₂ bond length in the pyrazolylborate- ([Tp^{Ph,Me}]Zn(CH₂CN)]; Tp^{Ph,Me} = hydrotris((5,3-methylphenyl-pyrazolyl)borate) 2.052(3) Å)[19a] and PMDTA-supported zinc cyanomethanide and (PMDTA = N,N,N',N'',N''-pentamethyldiethylenetriamine, 1.991(6) Å) reported.[19b] The C≡C bond length in **3** (1.207(3) Å) is longer than that in free phenylacetylene (1.183(2) Å) due to the donation of π-electron to zinc vacant orbitals. The Zn–C bond length in compound **3** (1.9519(17) Å) lies within the range observed for the monomeric [{(dipp)NacNac}ZnC≡CPh] (1.906(2) Å) ((dipp)NacNac = 2-{(2,6-diisopropyl-phenyl)amino}-4-{(2,6-diisopropylphenyl)

imino}pent-2-enyl).[20] In the IR spectrum of compound 2 a stretching band at ν(CN) = 2193 cm^{-1} indicates the presence of a terminal C≡N group.

In analogy to the synthesis of 1 through protonation of one of the Cp* ligands in Cp*Zn–ZnCp*, we attempted to protonate both Cp* ligands by reacting with 2 equivalents of the acid [(Me$_4$TACD)H][BAr$_4^{Me}$]. This only led to the formation of zinc(I) cation 1 along with unreacted acid. Recently, we reported that the zinc–zinc bond of zinc(I) cation [(TEEDA)Zn–ZnCp*][BAr$_4^{F}$] can cleave dihydrogen in a heterolysis, similar to a frustrated Lewis acid–base type activation.[8] When the reaction of compound 1 was carried out with a large excess (5 equivalents) of HBpin in acetonitrile at 60 °C for 3 days, the zinc(I)–zinc(I) dication [(Me$_4$TACD)Zn–Zn(Me$_4$TACD)][BAr$_4^{Me}$]$_2$ (4) was formed along with Cp*H, zinc metal, and B$_2$pin$_2$ (Scheme 3). Compound 4 was isolated in 30% yield (based on (Me$_4$TACD)Zn) and characterized in the solution state using multinuclear NMR spectroscopy and in the solid state using single crystal XRD studies.

In the ^{1}H NMR spectrum of compound 4, all the Me$_4$TACD protons (δ 2.33–2.51 ppm (CH$_2$) and δ 2.20 ppm (CH$_3$)) are deshielded compared to those in 1 (δ 2.14–2.31 ppm (CH$_2$) and δ 2.11 ppm (CH$_3$)) due to the increase in the cationic charge of the zinc centers. ^{13}C NMR spectra show all the corresponding signals for the Me$_4$TACD ligand and borate counterion. Compound 4 crystallizes in the orthorhombic space group Pbca with one ion pair in the asymmetric unit. The dinuclear structure of 4 with a zinc(I)–zinc(I) distance of 2.4860(6) Å was confirmed using single crystal XRD diffraction (Fig. 2a). Due to the higher coordination number in 4, the zinc–zinc distance is significantly longer than the zinc–zinc bond in the reported dications of the type [Zn$_2$(L$_6$)]$^{2+}$ [Zn$_2$(dmap)$_6$][Al{OC(CF$_3$)$_3$}$_4$]$_2$ (2.419(2) Å)[6a] and [Zn$_2$(thf)$_6$][BAr$_4^{F}$] (2.363(2) Å).[6b] As can be seen from the space-filling model (Fig. 2b), the two 9-electron [Zn(Me$_4$TACD)]$^+$ units are closely meshed and the two Me$_4$TACD ligands adopt a staggered conformation (Fig. 2c). Notably, both ligands show $\delta\delta\delta\delta$ or $\lambda\lambda\lambda\lambda$ conformation of the CH$_2$CH$_2$ units and the overall molecular symmetry of the homochiral dimer corresponds to the rare pointgroup D_4.

To provide further insight into the bonding in compounds 1 and 4, DFT calculations were performed at the B3PW91 level of theory. Gas phase optimized structure agrees well with the experimentally determined structures of 1 and 4 from X-ray diffraction studies. The LUMO is mainly located on the Me$_4$TACD ligand in both compounds. The zinc–zinc bond in compound 1 constitutes the HOMO−2, while the HOMO is localized on Zn–Cp* bond. In contrast, the HOMO is mainly localized on the zinc–zinc bond in compound 4 (Fig. 3). This is consistent with the apparent longer zinc–zinc bond in
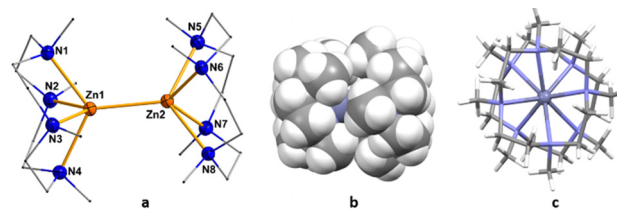

Fig. 2 (a) Left: Cationic part of the molecular structure of compound 4. The anion part [BAr$_4^{Me}$] and all H atoms are omitted for clarity. Displacement parameters are shown at 30% probability; selected interatomic distances [Å] and angles [°]: Zn1–N1 2.378(3), Zn1–N2 2.337(3), Zn1–N3 2.390(3), Zn1–N4 2.326(3), Zn1–Zn2 2.4860(6), Zn2–N5 2.480(3), Zn2–N6 2.291(3), Zn2–N7 2.463(3), Zn2–N8 2.278(3); N1–Zn1–N2 76.31(11), N1–Zn1–N3 120.82(11), N1–Zn1–N4 75.92(11), N1–Zn1–Zn2 120.99(8), N2–Zn1–Zn2 119.19(8), N3–Zn1–Zn2 118.18(8), N4–Zn1–Zn2 119.86(8). (b) Middle: Space filling model of 4. (c) Right: View of 4 along the Zn–Zn axis, highlighting the D_4 symmetry.

compound 4 (2.4860(6) Å) compared to 1 (2.3510(3) Å). Moreover, the presence of HOMO contribution in Zn–Cp* moiety goes in line with its reaction with the acidic proton of CH$_3$CN and HC≡CPh for the formation of HZnCp*.

The mechanism for the formation of 4 remains obscure. It seems plausible that HBpin may act as a hydride transfer reagent to provide short-lived zinc hydride and boryl species as intermediates during the formation of 4 with elimination of Zn, Cp*H, and B$_2$Pin$_2$. We have previously reported somewhat unstable Zn(I) hydridoborate species [(TEEDA)Zn(HBPh$_3$)–ZnCp*].[16] The formation of zinc(II) hydrides from HBpin was reported by Ingleson et al.[21] However, the zinc(II) hydride cation [(Me$_4$TACD)ZnH]$^+$, previously isolated as [(Me$_4$TACD)ZnH][HBPh$_3$][16] is stable with respect to dehydrocoupling. Xu et al. reported that the dehydrocoupling of zinc(II) hydride with a tridentate L$_2$X-type ligand forms the zinc(I)–zinc(I) bonded complex, but the reaction requires the presence of catalytic [Ni(CO)$_2$(PPh$_3$)$_2$] or stoichiometric [Pd(PPh$_3$)$_4$].[22] At this point, however, we cannot exclude other mechanistic pathways for the formation of 4, including radical intermediates.[22d,23]

In conclusion, we have prepared hypervalent zinc(I) complexes that contain the L$_4$-type macrocycle Me$_4$TACD 1 and 4. While the heteroleptic complex 1 can be accessed by protonolysis of dizincocene Cp*Zn–ZnCp* using the conjugate acid of Me$_4$TACD, the homoleptic complex 4 was only obtained by the treatment of 1 with the hydride reagent HBpin in a somewhat complicated reaction. The reaction of 1 with activated hydrocarbons acetonitrile (pK_a = 25) and phenylacetylene (pK_a = 29) suggests that C–H bond cleavage by the dinuclear zinc(I)–zinc(I) complexes can occur by a polarized zinc(I)–zinc(I) bond, possibly
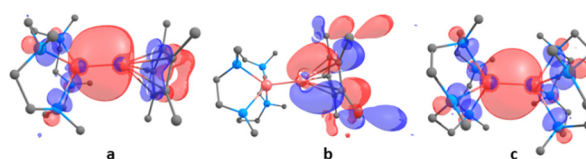

Fig. 3 (a) HOMO−2 for compound 1. (b) HOMO for compound 1. (c) HOMO for compound 4.

in the presence of a Brønsted base. While C–H bond activation has been reported for d-block transition metals,[24] zinc(I) complexes appear to show similar reactivity with relevance to C–H bond functionalization.[10]

We thank Dr Louis J. Morris for helpful discussions.

Data availability

The data supporting this article have been included as part of the ESI.†

Conflicts of interest

There are no conflicts to declare.

Notes and references

1 (a) I. Resa, E. Carmona, E. Gutierrez-Puebla and A. Monge, *Science*, 2004, **305**, 1136–1138; (b) A. Grirrane, I. Resa, A. Rodriguez, E. Carmona, E. Alvarez, E. Gutierrez-Puebla, A. Monge, A. Galindo, D. del Rio and R. A. Andersen, *J. Am. Chem. Soc.*, 2006, **129**, 693–703.
2 (a) M. L. H. Green and G. Parkin, *J. Chem. Educ.*, 2014, **91**, 807–816; (b) J. B. Jensen, *J. Chem. Educ.*, 2003, **80**, 952–961.
3 Z. Zhu, M. Brynda, R. J. Wright, R. C. Fischer, W. A. Merrill, E. Rivard, R. Wolf, J. C. Fettinger, M. M. Olmstead and P. P. Power, *J. Am. Chem. Soc.*, 2007, **129**, 10847–10857.
4 Y. Wang, B. Quillian, P. Wei, H. Wang, X.-J. Yang, Y. Xie, R. B. King, P. V. R. Schleyer, H. F. Schaefer and G. H. Robinson, *J. Am. Chem. Soc.*, 2005, **127**, 11944–11945.
5 K. Freitag, H. Banh, C. Ganesamoorthy, C. Gemel, R. W. Seidelb and R. A. Fischer, *Dalton Trans.*, 2013, **42**, 10540–10544.
6 (a) S. Schulz, D. Schuchmann, I. Krossing, D. Himmel, D. Bläser and R. Boese, *Angew. Chem., Int. Ed.*, 2009, **48**, 5748–5751; (b) H. Banh, C. Gemel, R. W. Seidelb and R. A. Fischer, *Chem. Commun.*, 2015, **51**, 2170–2172.
7 (a) M. L. H. Green and G. Parkin, *Dalton Trans.*, 2016, **45**, 18784–18795; (b) R. H. Crabtree, *Chem. Soc. Rev.*, 2017, **46**, 1720–1729.
8 P. Mahawar, T. Rajeshkumar, T. P. Spaniol, L. Maron and J. Okuda, *Inorg. Chem.*, 2024, **63**, 8493–9501.
9 J. T. Boronski, A. E. Crumpton, A. F. Roper and S. Aldridge, *Nat. Chem.*, 2024, **16**, 1295–1300.
10 (a) I. L. Fedushkin, O. V. Eremenko, A. A. Skatova, A. V. Piskunov, G. K. Fukin, S. Y. Ketkov, E. Irran and H. Schumann, *Organometallics*,
2009, **28**, 3863–3868; (b) R. K. Sahoo, S. Rajput, A. G. Patro and S. Nembenna, *Dalton Trans.*, 2022, **51**, 16009–16016; (c) R. K. Sahoo, A. G. Patro, N. Sarkar and S. Nembenna, *ACS Omega*, 2023, **8**, 3452–3460; (d) T. Li, S. Schulz and P. W. Roesky, *Chem. Soc. Rev.*, 2012, **41** 3759–3771.
11 J. H. Coates, D. A. Hadi and S. F. Lincoln, *Aust. J. Chem.*, 1982, **35**, 903–909.
12 (a) F.-G. Fontaine and V. Desrosiers, *Synthesis*, 2021, 4599–4613; (b) C. Jiang, O. Blacque and H. Berke, *Organometallics*, 2010, **29**, 125–133; (c) J. Guo, Ma Yan and D. W. Stephan, *Org. Chem. Front.*, 2024, **11**, 2375–2396.
13 (a) J. Dyke, W. Levason, M. E. Light, D. Pugh, G. Reid, H. Bhakhoa, P. Ramasami and L. Rhyman, *Dalton Trans.*, 2015, **44**, 13853–13866; (b) H. Bhakhoa, L. Rhyman, E. P. Lee, D. K. W. Mok, P. Ramasami and J. M. Dyke, *Dalton Trans.*, 2017, **46**, 15301–15310; (c) P. Ghana and J. Okuda, *Bull. Jpn. Soc. Coord. Chem.*, 2021, **77**, 37–45.
14 L. J. Morris, P. Ghana, T. Rajeshkumar, A. Carpentier, L. Maron and J. Okuda, *Angew. Chem., Int. Ed.*, 2022, **61**, e202114629.
15 D. Schuhknecht, T. P. Spaniol, L. Maron and J. Okuda, *Angew. Chem., Int. Ed.*, 2020, **59**, 310–314.
16 F. Ritter, L. J. Morris, K. N. McCabe, T. P. Spaniol, L. Maron and J. Okuda, *Inorg. Chem.*, 2021, **60**, 15583–15592.
17 B. Li, K. Huse, C. Wölper and S. Schulz, *Chem. Commun.*, 2021, **57**, 13692–13695.
18 (a) P. Jochmann and D. W. Stephan, *Angew. Chem., Int. Ed.*, 2013, **52**, 9831–9835; (b) P. Jochmann and D. W. Stephan, *Chem. – Eur. J.*, 2014, **20**, 8370–8378.
19 (a) H. Brombacher and H. Vahrenkamp, *Inorg. Chem.*, 2004, **43**, 6054–6060; (b) P. Mahawar, T. Rajeshkumar, T. P. Spaniol, L. Maron and J. Okuda, *Chem. – Eur. J.*, 2024, **30**, e202401262.
20 J. Prust, H. Hohmeister, A. Stasch, H. W. Roesky, J. Magull, E. Alexopoulos, I. Usón, H.-G. Schmidt and M. Noltemeyer, *Eur. J. Inorg. Chem.*, 2002, 2156–2162.
21 M. Uzelac, K. Yuan, G. S. Nichol and M. L. J. Ingleson, *Dalton Trans.*, 2021, **50**, 14018–14026.
22 (a) S. Jiang, Y. Cai, A. Carpentier, I. del Rosal, L. Maron and X. Xu, *Chem. Commun.*, 2021, **57**, 13696–13699; (b) M. Chen, S. Jiang, L. Maron and X. Xu, *Dalton Trans.*, 2019, **48**, 1931–1935; (c) S. Jiang, M. Chen and X. Xu, *Inorg. Chem.*, 2019, **58**, 13213–13220; (d) S. Xu, Q. Wang, T. Rajeshkumar, S. Jiang, L. Maron and X. Xu, *J. Am. Chem. Soc.*, 2024, **146**, 19590–19598.
23 Y. L. Phang, J.-K. Jin, F.-L. Zhang and Y.-F. Wang, *Chem. Commun.*, 2024, **60**, 4275–4289.
24 (a) T. Tanabe, M. E. Evans, W. W. Brennessel and W. D. Jones, *Organometallics*, 2011, **30**, 834–843; (b) Y.-H. Chang, K. Takeuchi, M. Wakioka and F. Ozawa, *Organometallics*, 2015, **34** 1957–1962.